Journal of Microscopy and Ultrastructure 2 (2014) 104–116

Contents lists available at ScienceDirect

Journal of Microscopy and Ultrastructure

journal homepage: www.elsevier.com/locate/jmau

Original Article

Morphology, ultrastructure and immunocytochemistry of *Hypnea cervicornis* and *Hypnea musciformis*-(Hypneaceae, Rhodophyta) from the coastal waters of Ceará, Brazil

Thaiz B.A. Rangel Miguel[a], Eder C. Schmidt[b], Zenilda L. Bouzon[b], Fernando E.P. Nascimento[a], Maura Da Cunha[c], Saulo F. Pireda[c], Kyria S. Nascimento[d], Celso S. Nagano[a], Silvana Saker-Sampaio[a], Benildo S. Cavada[d], Emilio C. Miguel[d], Alexandre H. Sampaio[a,*]

[a] *Universidade Federal do Ceará, Departamento de Engenharia de Pesca, Laboratório de Biotecnologia Marinha – BioMar-Lab, Fortaleza, Ceará, Brazil*
[b] *Universidade Federal de Santa Catarina, Departamento de Biologia Celular, Laboratório de Biologia Celular Vegetal, Embriologia e Genética, Florianópolis, Santa Catarina, Brazil*
[c] *Universidade Estadual do Norte Fluminense Darcy Ribeiro, Centro de Biociências e Biotecnologia, Laboratório de Biologia Celular e Tecidual, Campos dos Goytacazes, Rio de Janeiro, Brazil*
[d] *Universidade Federal do Ceará, Departamento de Bioquímica e Biologia Molecular, Laboratório de Moléculas Biologicamente Ativas – BioMol-Lab, Fortaleza, Ceará, Brazil*

ARTICLE INFO

Article history:
Received 19 February 2014
Received in revised form 26 March 2014
Accepted 30 March 2014
Available online 24 April 2014

Keywords:
Hypnea musciformis lectin
Hypnea cervicornis lectin
Ultrastructure
Algae morphology
Lectin subcellular localization

ABSTRACT

Based on their morphological and physiological features, red algae comprise a complex and variable group of multiple genera, including *Hypnea.* In particular, the genus *Hypnea* J.V. Lamouroux (Cystocloniaceae, Rhodophyta) consists of approximately 54 species, including *Hypnea cervicornis* and *H. musciformis*. Lectins were described for both species; however, the localization of these proteins is still unclear. Therefore, this work aimed to characterize the morphology and ultrastructure of *Hypnea cervicornis* and *H. musciformis*, as well as localize their lectins at the subcellular level. Samples were collected at Praia do Pacheco (Fortaleza-CE) and processed for light, scanning and transmission electron microscopy, in addition to immunocytochemistry. The studied species presented cortical cell layers, subcortical cells and medullary cells. Based on ultrastructural analysis, these species presented vacuolated cortical cells, with a dense cytoplasm containing chloroplasts. The cell wall consisted of concentric microfibrils embedded in an amorphous matrix. Immunochemistry analysis showed the expression of lectins in the cytoplasm and cell walls. While the structure of the studied algae was similar to the description of other species of the genera under different conditions, this is the first record of algae lectin localization.

1. Introduction

Red algae vary in many aspects, including structural. For example, these organisms can present thalli that vary from flattened to foliose, variously lobed and deeply incised, with heights up to 4 cm and widths from

* Corresponding author at: Marine Biochemistry Laboratory – BioMar-Lab, BioMol-Lab, Department of Fishing Engineering, Federal University of Ceará, P.O. Box 6043, 60440-970 Fortaleza, Ceará, Brazil.
Tel.: +85 3366 9728; fax: +85 3366 9417.
E-mail address: alexholandasampaio@gmail.com (A.H. Sampaio).

http://dx.doi.org/10.1016/j.jmau.2014.03.004
2213-879X/

0.5–2 cm, narrowing to short stalks of 1–2 mm in width, and a slightly expanded basal pad with a gelatinous texture, such as *Predaea feldmannii* Børgesen (Nemastomataceae, Rhodophyta) [1]. *Hypnea flexicaulis* Y. Yamagishi & M. Masuda (Cystocloniaceae, Rhodophyta) has been described as brownish-red or greenish-yellow, with fleshy or subcartilaginous structures 5–35 cm in height, exhibiting 4–6 large, pyriform, radially elongated (150–200 μm) medullary cells (200–300 μm high) surrounding a small axial cell that is 40–60 μm in diameter [2].

The ultrastructure of chloroplasts, which is also a variable characteristic, can have taxonomic value in algae. Thylakoid arrangement of different phyla is one of the most important features corroborating traditional taxonomy [3]. In red algae, the thylakoids are free within the chloroplasts [4]. The phycobiliproteins are localized into phycobilisomes on the surface of thylakoids [5]. Another characteristic structure of some red macroalgae is the pit connection. The pit plug, which fills the pit connection, is composed of a slightly granular, electron-dense material. This plug is covered by two proteinaceous membranes and fills the channel between the daughter cells that results from partial cytokinesis. However, although the pit connections maintain contact between daughter cells, no cytoplasmic continuity is permitted because the plugs are generally deposited in the septal aperture shortly after furrowing ceases [6]. Among red algae species of *Hypnea* genus are noted.

The genus *Hypnea* J.V. Lamouroux (Cystocloniaceae, Rhodophyta) includes approximately 54 species, which are abundant in intertidal and subtidal zones of tropical and warm temperate waters. This genus is distinguished by brownish-red or greenish-yellow branched thalli with short lateral branchlets [7,8].

Hypnea structure is complicated by a high degree of morphological plasticity, which results in evident differences among individuals of the same species [8]. Molecular and ultrastructural data can be useful in species taxonomy [2], not only to distinguish species of the same genus, but also to differentiate *Hypnea* from other genera [9]. Among *Hypnea* species are found two marine algae, *Hypnea cervicornis* J. Agardh and *Hypnea musciformis* (Wulfen) J.V. Lamouroux, which were selected for this study.

Previous studies have shown that *H. musciformis* exhibits aquaculture potential for carrageenan production [10–13]. Moreover, marine algae from the genus *Hypnea* have been reported as an important source of biologically active molecules, such as lectins. These molecules have been shown to agglutinate mouse FM3A tumor cells [14], and they present antinociceptive and anti-inflammatory activity [10,11]. The chemical aspects of lectins of selected species have been well characterized by our group, e.g., lectin isolation in *H. musciformis* [15] and *H. cervicornis* [16].

Lectins are nonimmune proteins that reversibly bind to carbohydrates. These proteins have been identified in all kingdoms of life, from viruses to animals and from algae to plants [17]. Marine algal lectins are especially interesting for biological applications because they have lower molecular weights compared to most plant lectins. In addition, small algal lectin molecules can be less antigenic than the larger plant lectins [18].

The physiological role of lectins is not completely understood; however, higher plant lectins are described as defense [19] or reserve [20] proteins. Algal lectins might be involved in cell-to-cell recognition during fertilization in *Antithamnion sparsum* Tokida (Ceramiaceae, Rhodophyta) [21], protoplast regeneration in *Bryopsis hypnoides* J.V. Lamouroux (Bryopsidaceae, Chlorophyta) [22], and protoplast assembly in *Codium fragile* (Suringar) Hariot (Bryopsidaceae, Chlorophyta) [23]. However, the subcellular localization of macroalgal lectins has not been determined. Understanding lectin subcellular localization is an important step to a complete elucidation of the role of this molecule. Therefore, this work aimed to describe the morphology and ultrastructure of *Hypnea cervicornis* in comparison to *H. musciformis* and characterize the expression of lectins using immunochemistry.

2. Material and methods

2.1. Plant material

In April 2011, algae samples were collected at Praia do Pacheco (CE) (3°41.091′ S 38°38.130′ W) at low tide at mesolittoral zone in the water column with a few centimeters. The material was taken to the laboratory and photographed.

2.2. Scanning electron microscopy

Sample fragments of approximately 1 cm were immediately fixed overnight in a solution containing 2.5% glutaraldehyde and 4.0% formaldehyde diluted in a 0.1 M sodium cacodylate buffer. The material was post-fixed in 1.0% osmium tetroxide for 2 h and dehydrated in a graded acetone series (30°, 50°, 70°, 90°, 100°, 100° and 100° 1 h each step). For scanning electron microscopy, the samples were critical point dried with CO_2 (CPD 030, Balzers), sputter-coated with 10 nm gold (Q 150t ES, Quorum), and observed under a scanning electron microscope (DSEM 962-ZEISS/Inspect 50-FEI) at 10–20 kV.

2.3. Light microscopy

For light microscopy, the samples were fixed, post-fixed, and dehydrated as described for scanning electron microscopy. Subsequently, the material was infiltrated and embedded in the epoxy resin Epon (Polybed) for three days, followed by 48 h at 60 °C for polymerization. Sections 0.5 μm thick were obtained using an ultramicrotome (Reicheit Ultracut S) and stained with toluidine blue (1.0% aqueous solution). The slides were sealed with Entellan® and coverslips and examined using an Axioplan microscope (Zeiss). Images were captured with a Cannon Power Shot 14 megapixel camera. The images were processed using Axiovision 4.8 software (Zeiss).

2.4. Transmission electron microscopy

Algal fragments were fixed, post-fixed, dehydrated, and embedded as described previously. Ultrathin sections (60 nm) were obtained with an ultramicrotome,

collected on 300-mesh grids, and contrasted with 1.0% uranyl acetate, followed by 5.0% lead citrate [24], for transmission electron microscopy observation (EM 900, Zeiss) at 80 kV.

2.5. Immunodiffusion assay

Immunochemistry studies were performed to establish the relationships among HML (*Hypnea musciformis* lectin), the anti-HML antibody, ConBr (*Canavalia brasiliensis* lectin) and BSL (*Bryothamnion seaforthii* lectin). The IgY anti-HML antibody was obtained commercially at IgYBiotecnologia (Cambém, PR, Brazil). Immunodiffusion tests were performed overnight on 1% agarose gels prepared with 0.05 M phosphate buffer, pH 8.0, containing 0.02% sodium azide. Subsequently, the agarose gels were stained with an aqueous solution containing 50% methanol, 0.05% Coomassie Blue R, and 10% acetic acid. After staining, the gels were destained in water and photographed.

2.6. Immunohistochemistry assay (LM)

Algal fragments were fixed in 0.01% glutaraldehyde and 4% formaldehyde in a 0.2 M sodium cacodylate buffer, pH 7.4, dehydrated in methanol and embedded in LR Gold resin. Sections 0.5 μm thick were obtained using an ultramicrotome (Reicheit Ultracut S), mounted on slides and subjected to immunocytochemical tests.

Slides were processed using the Silver Enchancing Kit for Light and Electron Microscopy (BBISolutions, UK), following the manufacturer's instructions. Anti-lectin IgY primary antibodies were commercially obtained (10 mg/mL-IgY; IgYBiotecnologia, Brazil) and utilized in a 1:150 dilution. Secondary antibody was utilized in a 1:200 dilution. The images were processed as described for light microscopy.

2.7. Immunocytochemistry assay (EM)

Algae fragments obtained as described for scanning electron microscopy were fixed with 4% formaldehyde and 0.05% glutaraldehyde in 0.2 M sodium cacodylate buffer, dehydrated in a graded acetone series (50–100%), and embedded in LR Gold resin according to the manufacturer's instructions. Ultra-thin sections were obtained using a diamond knife on an ultramicrotome (RMC, USA) and collected on 300 mesh formvar-covered Ni grids.

Immunolabeling was carried out at room temperature. The sections were incubated in ammonium chlorite, pH 8.0, and washed in PBS/BSA. Then, the sections were incubated for 1 h with anti-lectin IgY primary antibodies (10 mg/mL-IgY; Biotecnologia, Brazil) 1:150 IgY to PBS.

After rinsing in PBS, the sections were labeled for 1 h on drops of donkey antibody against chicken IgY gold conjugate (12 nm diameter gold particles, Abcam), diluted 1:200 in PBS. The sections were washed in PBS, rinsed in water and stained with uranyl acetate (20 min), followed by lead citrate (2 min) [24]. Control grids to detect nonspecific immunolabeling were made using IgY from nonimmunized chicken or by omitting the primary antibodies. Observation and documentation were performed as previously described for transmission electron microscopy.

3. Results

3.1. Morphology of the thalli

H. cervicornis thalli were cylindrical, brownish-red, and approximately 500 μm in diameter (Fig. 1a), with alternate spiral branching at angles of 45°–90° with approximately 4 ramifications per centimeter (Fig. 1b). Some branches were highly curved at the tip, resulting from abrupt abaxial bending. In contrast, *H. musciformis* thalli were cylindrical light brown structures approximately 600 μm in diameter (Fig. 1c), with alternate branching at close to 45° angles with approximately 8 ramifications per centimeter (Fig. 1d), and hook-ended.

3.2. Observation under light microscope (LM)

The transverse sections of *H. cervicornis* showed 1–3 cortical cell layers, with 1–2 isodiametric subcortical cells, larger than the cortical cells, and 1–2 radially elongated medullary cells (Fig. 2a). The cortical cells were small at approximately 12 μm, with dense cytoplasm, evident nuclei, and large vacuoles (Fig. 2b, c). The cell wall was thick (Fig. 2c). The subcortical cells, however, were more vacuolated compared with the cortical cells, with sizes varying from 40 to 60 μm in diameter and 40 to 50 μm in length, gradually increasing in size toward the medullary region (Fig. 2c). The medullary cells were isodiametric or radially elongated, with thin cell walls and large vacuoles, varying from 50 to 60 μm in diameter and 60 to 150 μm in length (Fig. 2d).

The transverse sections of *H. musciformis* showed 1–3 cortical cell layers, with 1–2 isodiametric subcortical cells and 4–6 irregular medullary cells (Fig. 2e). The cortical cells were small, measuring approximately 10 μm, with dense cytoplasm and a thick cell wall (Fig. 2f, g). Nuclei were not evident. The subcortical cells were larger than the cortical cells, measuring 30–50 μm in diameter and 30–60 μm in length, surrounded by a thick cell wall with large vacuoles (Fig. 2f, g). The medullary cells were bigger than the subcortical cells, measuring 40 and 50 μm in diameter and 50 and 90 μm in length, surrounded by a cell wall with lenticular thickness (Fig. 2h).

3.3. Observation under scanning electron microscope (SEM)

Under scanning electron microscopy, *H. cervicornis* presented cylindrical thalli (Fig. 3a) with blunt ramifications (Fig. 3b). A closer view revealed that the surface was ornamented (Fig. 3c). *H. musciformis* also presented cylindrical thalli (Fig. 3d), but with acute ramifications (Fig. 3e). Epiphytes were observed on the surface of the thalli (Fig. 3f).

Careful observation of the surface of the thalli revealed that epiphytes and mucilage were present on both species. *H. cervicornis* presented thalli with a rough tip, covered with mucilage (Fig. 3g). At the thallus midpoint, the mucilage exhibited a turgid surface (Fig. 3h). In

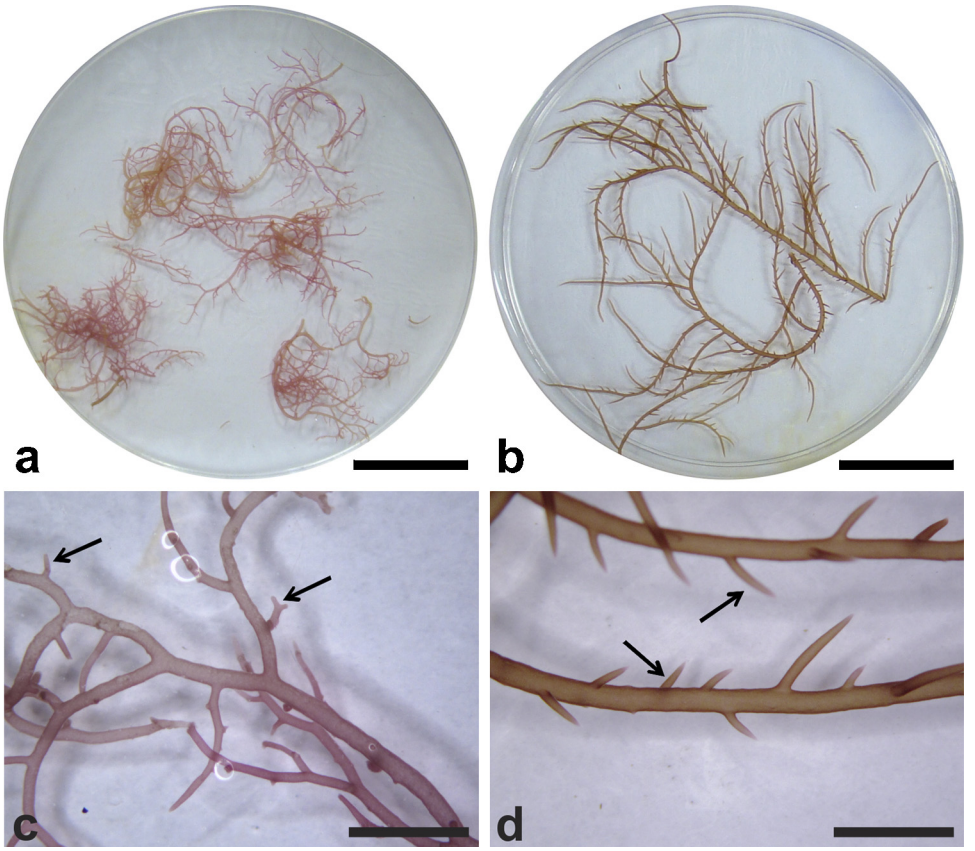

Fig. 1. General aspects of *Hypnea cervicornis* (a, b) and *H. musciformis* (c, d) thalli. a and c – Overview of thalli habitus; b and d – Detail of thalli. Arrows – thalli ramifications. Bars: a, c – 2 cm; b, d – 0.25 cm.

H. musciformis, the cortical cells were covered with mucilage (Fig. 3i); however, the thallus midpoint presented turgid cells (Fig. 3j).

3.4. Observation under transmission electron microscopy (TEM)

Under transmission electron microscopy *H. cervicornis* showed the presence of vacuolated cortical cells with a dense cytoplasm filled with chloroplasts (Fig. 4a). These cells were surrounded by a thick cell wall (Fig. 4b). Epiphytes were observed on the mucilage-covered surface (Fig. 4b). The cell wall was formed by concentrically arranged microfibrils embedded in an amorphous matrix, which consisted of sulfated polysaccharides called carrageenans (Fig. 4c). The subcortical cells presented a peripheral thin cytoplasm and large vacuoles (Fig. 4c). It was possible to observe vacuoles and large and elongated chloroplasts.

H. musciformis showed cortical and subcortical cells with a dense cytoplasm containing chloroplasts with similar structures (Fig. 4d, e) and small vacuoles. However, the cortical and subcortical cells were surrounded by a thick cell wall comprised of concentrically arranged microfibrils (Figs. 4d–h). In addition, the cortical cells were associated with the subcortical cells through pit connections (Fig. 4f). The chloroplasts were also observed in the medullary cells (Fig. 4g). Morphological data are summarized in Table 1.

3.5. Immunodiffusion assay

The anti-HML (1 mg/mL or 2 mg/mL) antibody showed no immunological activity against *Canavalia brasiliensis* lectins (ConBr) (Fig. 5a, b), *Bryothamnion seafortii* lectins (BS) (Fig. 5c, d) at different protein concentration (2, 1, 0.5, 0.25 or 0.12 mg/mL) or Albumina (negative control 2 mg/mL; dot A on Fig. 5e–h). However, the anti-HML (2 mg/mL) antibody was immunoreactive against purified HML and HCL at 2, 1, 0.5 and 0.25 mg/mL (Fig. 5e–g). At 1 mg/mL, anti-HML exhibited complete immunological identity with HML and HCL at concentrations of 2, 1 and 0.5 mg/mL (Fig. 5f, h).

3.6. Immunohistochemistry assay

The results of the immunohistochemistry assay revealed that HML was expressed in different cellular regions of *H. musciformis* tissue. The expression of HML in the external cell wall was apparently stronger than in other regions, such as the internal cell wall and cytoplasm. HML expression was also evident in the cell walls of

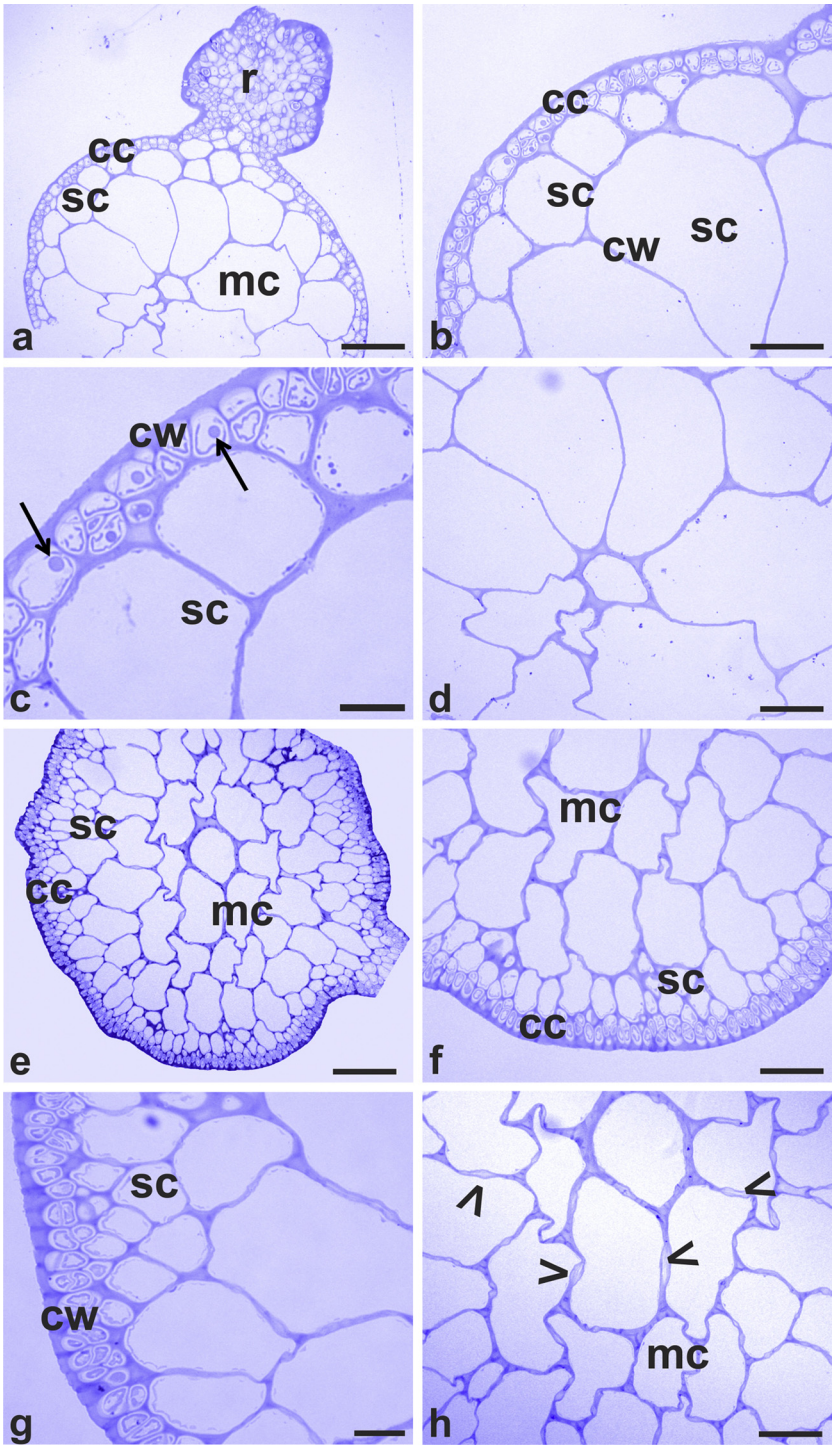

Fig. 2. Light microscopy of *Hypnea cervicornis* (a–d) and *H. musciformis* (e–f) thalli transverse section. a – Transverse section of the thallus, showing ramifications. Note: 1–2 layers of cortical cells (cc) followed by subcortical cells (sc). The medullary region is formed by large medulary cells (mc) with vacuoles; b – cortical cells and subcortical cells with thin cell walls; c – detail of the previous image. Note: cortical cells with dense cytoplasm and evident nuclei. Subcortical cells are smaller than medullary cells; d – detail of the central region showing medullary cells; e – transverse section of the thallus. Note: 1–2 layers of cortical cells followed by subcortical cells; f – cortical, subcortical and medullary cells; g – detail of the previous image. Note: cortical cells with dense cytoplasm and subcortical cells; h – detail of the central region, showing medullary cells. Note: the lenticular thickness of the cell wall. cc – cortical cells; sc – subcortical cells; mc – medullary cells; arrow – nuclei; r – thalli ramifications; arrowhead – lenticular thickness of the cell wall. Bars: a–e – 100 μm; b, c, f, g – 50 μm; d, h – 20 μm.

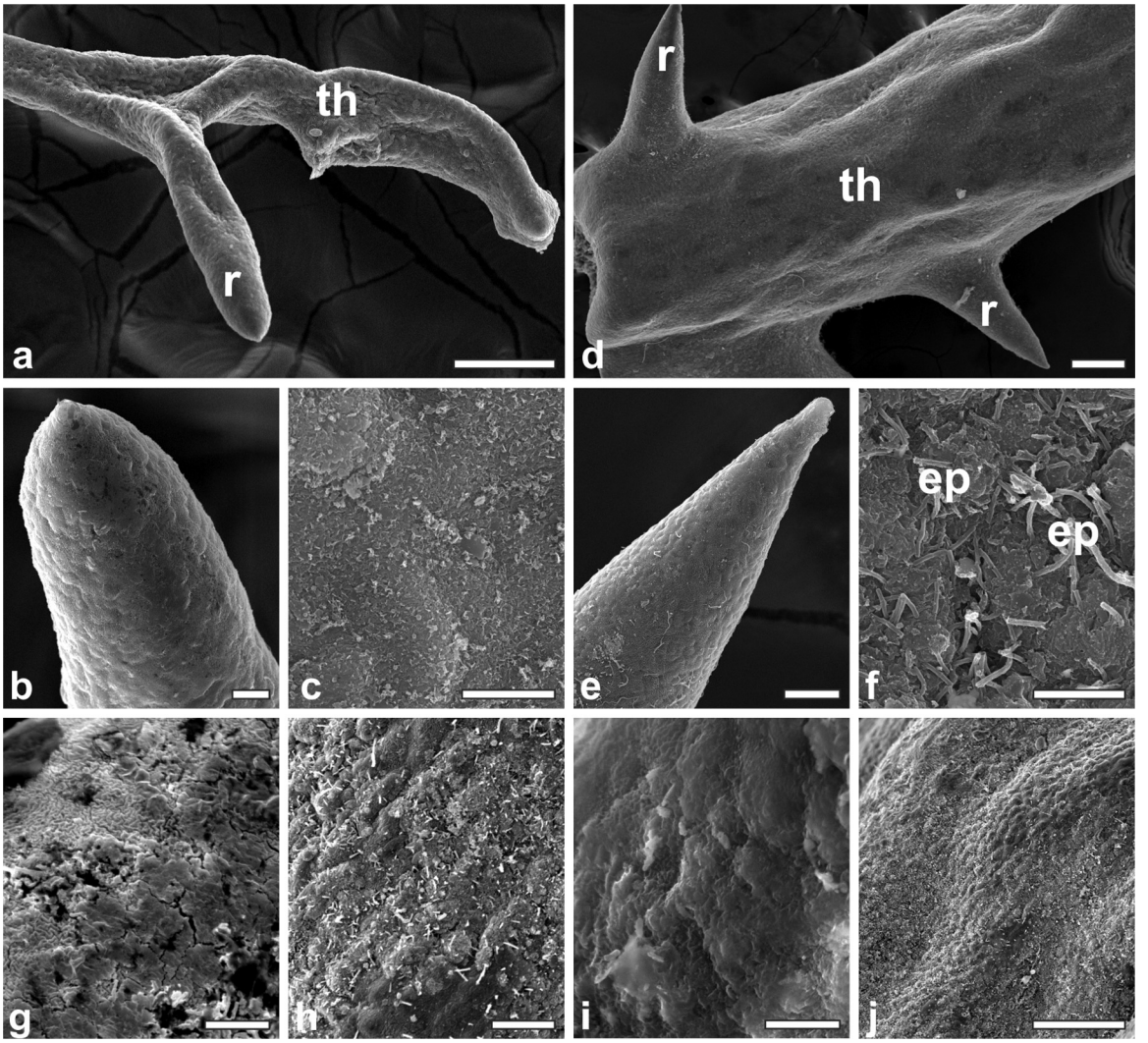

Fig. 3. Scanning electron microscopy of *Hypnea cervicornis* (a–c, g, h) and *H. musciformis* (d–f, i, j) thalli. a and d – General aspect of thalli; detail of blunt (b) and sharp (e) thalli ramifications. c and f – Algal surface. Note: epiphyte presence on f; g–j – Comparison of rough algal apex surface (g, h) and turgid surface at other regions of the thalli (i, j). th – thalli; r – ramifications; ep – epiphyte. Bars: a, b, e – 100 μm; d, h – 10 μm; c, f, g, i – 5 μm; j – 50 μm.

subcortical cells. No expression was observed in the vacuoles (Fig. 5i). In the cortical cells, HML was noted on the cell wall and cytoplasm, as revealed by homogeneous staining, except for the cell wall in contact with the exterior, where staining seemed to be stronger. In contrast, the vacuole presented no reaction. Subcortical cells exhibited staining on the cell wall and cytoplasm, but not on vacuoles. Medullary cells exhibited staining on the cell wall, but not on the cytoplasm or vacuole (Fig. 5i).

Except for the cortical cell walls in contact with the exterior, all stained regions presented similar intensity, indicating that HML is homogeneously distributed in tissues, but absent from the vacuole. The expression of HCL on *H. cervicornis* sections, as recognized by the same antibody, followed the same pattern (Fig. 5j); however, the antibody recognition was weaker. Control results did not reveal any staining (Fig. 5k, l).

3.7. Immunocytochemistry assay

The immunocytochemistry assay confirmed the immunohistochemistry results for both species. Control sections did not exhibit any impregnation of gold particles (Fig. 6a, f). HML immunolocalization in *H. musciformis* tissue revealed the presence of free protein in the cytoplasm and cell wall (Fig. 6a–e), but not in the vacuole. *Hypnea cervicornis* tissue revealed the same pattern (Fig. 6g–i), but with an apparently weaker protein–antibody affinity.

4. Discussion

The present work characterized the morphology of HC and HM under field conditions, without a period of adaptation or acclimatization under laboratory conditions. *H. cervicornis* and *H. musciformis* thalli were studied using different microscopy techniques. Careful observation of each

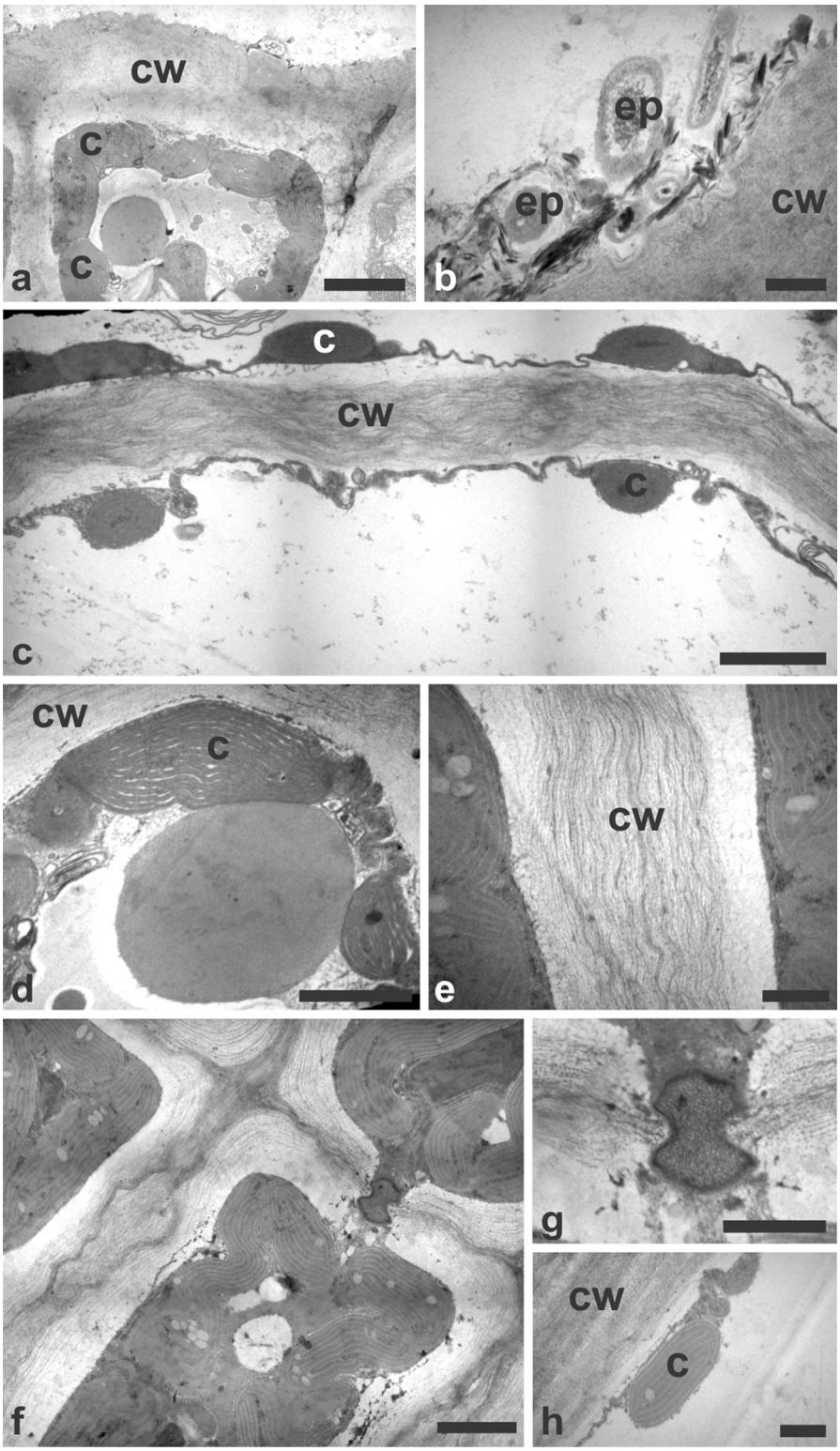

Fig. 4. Transmission electron microscopy of *Hypnea cervicornis* (a–d) and *H. musciformis* (e–h) thalli. a – Cortical cell, showing the cell wall (cw) and a dense cytoplasm, with many chloroplasts (c) and vacuoles. Note: cell wall organization; b – detail of epiphytes on the cell wall; c – cell wall of subcortical cells; d – detail of a subcortical cell evidencing chloroplast (c) and cell wall (cw); e – cell wall (cw) detail; f – cortical and subcortical cells. Note: the lenticular thickness, pit connections and abundant chloroplasts. Note arrow showing the lenticular thickness of the cell wall in f; g – detail of the pit connection; h – detail of the chloroplast in the subcortical cell. cw – cell wall; c – chloroplast; ep – epiphyte. Bars: a – 1 μm; b, e, h – 200 nm; c, d, f – 500 nm; g – 250 nm.

Table 1
Summary of the main characteristics of *Hypnea cervicornis* and *H. musciformis*.

	H. cervicornis	*H. musciformis*
General thalli aspects		
Morphology of the thalli	Cylindrical	Cylindrical
Thalli thickness	Approximately 500 μm	Approximately 600 μm
Collor of the thalii	Brownish-red	Light brown
Branching	Alternate spiral	Alternate spiral
Branching angle	45°–90°	45°
Number of ramifications (/cm)	Approximately 4	Approximately 8
Ramification tip	Blunt	Acute
Surface ornamentation	Yes	Yes
Epiphytes presence	Yes	Yes
Cell morphology		
Cortical cells number	1–3	1–3
Cortical cells size	12 μm	10 μm
Cortical cells shape	Isodiametric	Isodiametric
Subcortical cells number	1 or 2	1 or 2
Subcortical cells size	40–60/40–50 μm	30–50/30–60 μm
Subcortical cells shape	Isodiametric	Isodiametric
Medular cells number	1 or 2	4–6
Medular cells size	50–60/60–150 μm	40–50/50–90 μm
Medular cells shape	Radial elongated	Irregular
Cell ultrastructure		
Cortical cells ultrastructure	Vacuolated, dense cytoplasm, chloroplast presence, thick cell wall, formed by concentric microfibrills embbebed in an amorphous matrix	Low vacuolated, dense cytoplasm, chloroplast presence, thick cell wall, formed by concentric microfibrills embbebed in an amorphous matrix

species allowed the distinct characterization of their particular features.

The hook-ended thalli of *H. musciformis* are a remarkable characteristic of this species. Previous studies have identified other species with that feature, such as *H. flexicaulis* Y. Yamagishi & M. Masuda [2,25]. However, *H. chardoides-valentiae* (Rhodophyta, Gigartinales) [25] and *H. asiatica* P.J.L. Geraldino, E.C. Yang & S.M. Boo [26] do not present these structures, as confirmed in this study with *H. cervicornis*. The angle branches can also vary between species, being abrupt on *H. asiatica* P.J.L. Geraldino, E.C. Yang & S.M. Boo [26], 45°–150° (occasionally 180°) on *H. flexicaulis* Y. Yamagishi & M. Masuda, or 30°–90° on *H. chardoides* [25].

The mucilage texture observed under scanning electron microscopy can be associated with the internal layers of the analyzed region, as observed on *Gracilaria tikvahiae* McLachlan, which showed significant folding in the cortical cells. In contrast, the branch tips of *G. cornea* did not show surface tension [27]. Many factors affect the algal surface, as observed on *Corallina elongata* J. Ellis & Solander (Corallinales, Rhodophyta), where differences in cell wall thickness were detected in specimens obtained from hydrothermally active locations [28]. However, the surface texture could result from mucilage deposition on the cell wall, as observed on *H. cervicornis* and *H. musciformis* in the present study. Although mucilage deposition is common on reproductive structures [29], glycoprotein and/or sulfated polysaccharides can also be seen on vegetative cells [30,31].

Our results suggest that the relationship between epiphytes and algae is not parasitic because no epiphytes were observed to penetrate the outer cell wall. Thus, this relationship is likely to be a passive interaction, as described for *Kappaphycus alvarezii* (Doty) Doty ex P.C. Silva (Rhodophyta) [32], which is different from the structurally detailed parasitic interaction described for *Choreonema thuretii* (Bornet) F. Schmitz (Rhodophyta) [33] and cadmium-exposed *H. musciformis* [34].

The high degree of morphological variation within individual species, which may be chiefly influenced by the environmental factors in specific habitats, complicates species discrimination in *Hypnea* [25]. On the other hand, no significant variation was noted in species collected in different regions of Brazil and kept in under laboratory conditions [35].

Although similarities in the morphology of some *Hypnea* species have previously been described, some remarkable characteristics are different. *H. charoides-valentiae* [25] and *H. asiatia* P.J.L. Geraldino, E.C. Yang & S.M. Boo [26] exhibit thick cell walls, especially compared with *H. cervicornis*. The pit connections of *H. asiatia* are visible, even under optical microscopy [26], in contrast to species of the present study where the pit connections are visible only under electron microscopy. The main axis of *H. flexicaulis* Y. Yamagishi & M. Masuda is formed by a small number of cells [2] compared with the species of the present study.

The variations within algal cell structure reflect morphological variations. The structural differences in the apical, middle and basal thallus regions, as described in *Colpomenia sinuosa* (Mertens ex Roth) Derbès & Solier (Phaeophycota) [36], *Lobophora variegata* (J.V. Lamouroux) Womersley ex E.C. Oliveira (Phaeophycota) [37] and *Dictyopteris divaricata* (Okamura) Okamura (Phaeophycota) [38] were not observed in *H. cervicornis* or *H. musciformis* (data not shown) which both showed similar features of thallus morphology for the three regions. This variation, or lack of variation, must therefore be a genetic feature that is unrelated to the environment.

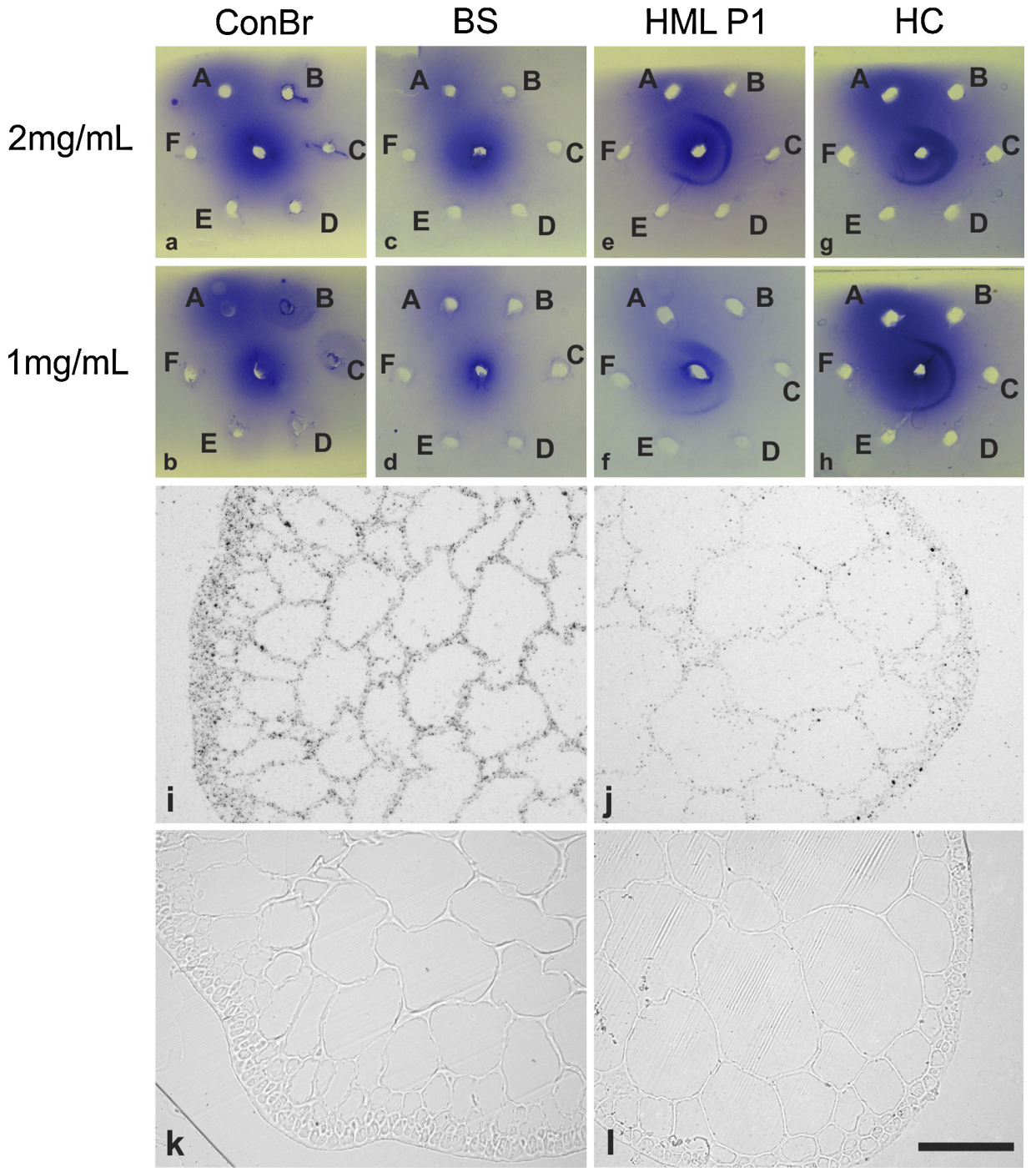

Fig. 5. Immunodiffusion of proteins against anti-HML antibody (a–h) and immunohistochemistry assay (i–l). Immunodiffusion of proteins against IgG anti-HML 2 mg/mL (a, c, e, g) or 1 mg/mL (b, d, f, h) against *Canavalia brasiliensis* lectin (ConBr) (a, b), *Bryothaminion seafortii* lectin (BS) (c, d), *Hypnea musciformis* lectin (HML P1) (e, f) and *H. cervicornis* lectin (HC) (g, h). Dots: Central – IgG-anti-HML P1; A – albumin 2 mg/mL; B – 2 mg/mL; C – 1 mg/mL; D – 0.5 mg/mL; E – 0.25 mg/mL and F – 0.012 mg/mL. Note: complete immunological identity (precipitation) on HML P1 and HC dots 2–5 (e–h). Immunohistochemistry assay of *H. musciformis* (i, k) and *H. cervicornis* (j, l). Note precipitation indicating lectin presence on cell walls and cytoplasm of cortical cells (i, j) compared to control (k, l). *H. musciformis* exhibited strong precipitation (j). Bar: 100 μm.

Ultrastructurally, the studied species presented typical red algal cells with cell wall consisting of a microfibrillar texture embedded in a more amorphous matrix [39]. When analyzed under transmission electron microscopy, *H. cervicornis* and *H. musciformis* showed a microfibrillar texture with microfibrils deposited in concentric layers with varying degrees of compression. Production of the fibrillar components of the cell wall is similar in many

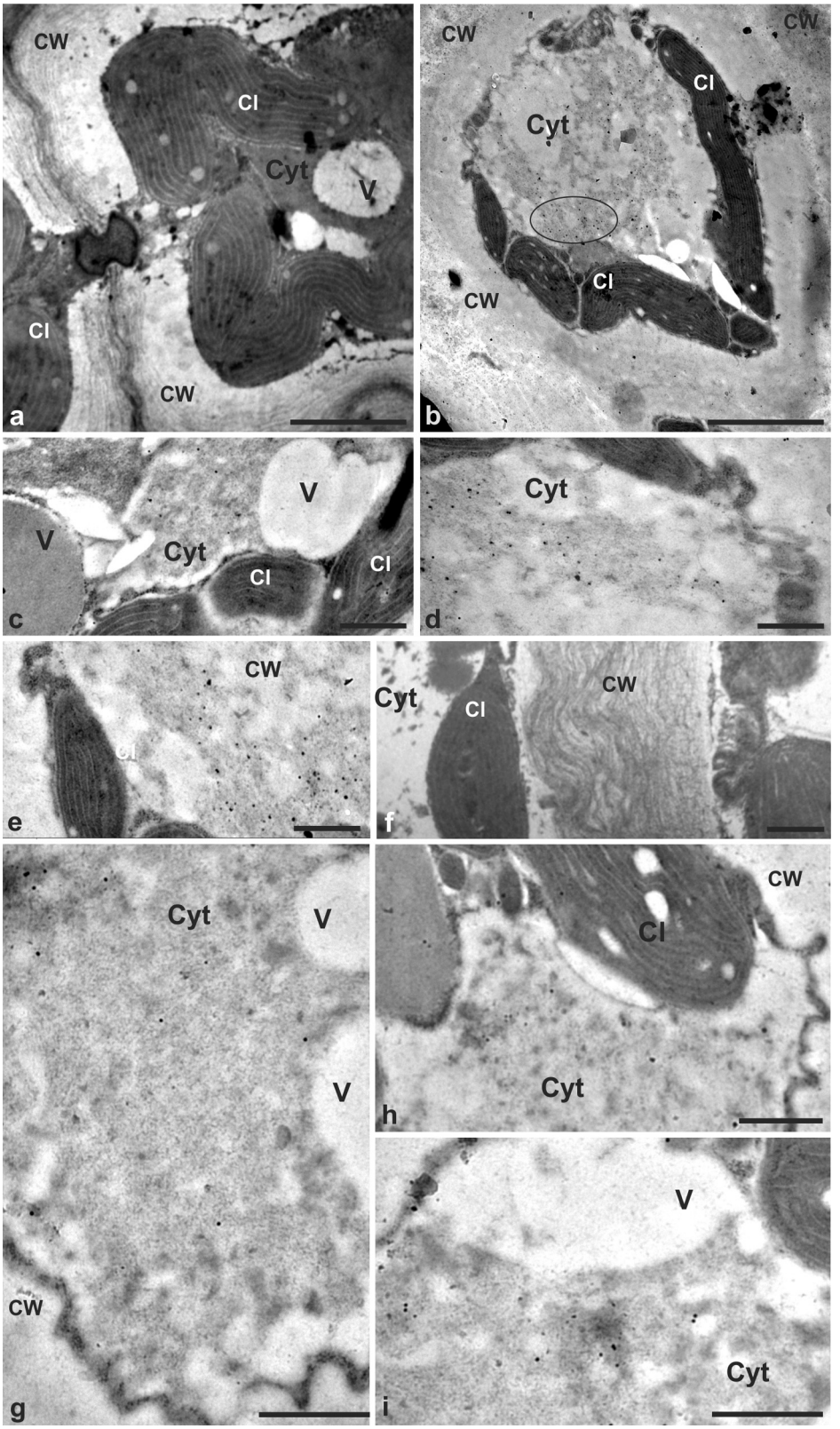

Fig. 6. Immunocytochemistry of *H. musciformis* (a–e) and *H. cervicornis* (f, i) thalli: lectin localization. a, f – Control experiments; no gold particles were noted. On the experimental images, gold particles were noted in both species in cytoplasm and cell wall, but not on vacuoles or chloroplasts. Bars: a, b – 1 μm; c–i – 250 nm.

red algae and seems to result from fibrous vacuoles, endoplasmic reticulum and the subsequent addition of vesicles derived from Golgi bodies [40].

The ultrastructure of other Rhodophyta, such as *Gracilaria tikvahiae* McLachlan and *G. cornea* J. Agardh (Gracilariales) [27], *Kappaphycus alvarezii* (Doty) Doty ex P.C. Silva (Gigartinales) [4,35], *Gracilariopsis tenuifrons* (C.J. Bird & E.C. Oliveira) Fredericq & Hommersand (Gracilariales) [34], and *Gelidium floridanum* W.R. Taylor (Gelidiales) [41] were described. The structural characteristics of studied species were, for the most part, noted in different algal groups, such as *Codium fragile* (Suringar) Hariot protoplasts (Chlorophyta) [23], *Padina gymnospora* (Kützing) Sonder (Ochrophyta) and *Cryptopleura ruprechtiana* (J. Agardh) Kylin (Rhodophyta). These remarkable features include the presence of a dense cytoplasm with small vacuoles and lipid bodies [42], as also noted in both *H. musciformis* and *H. cervicornis* in the present study.

In contrast to other species of red algae, no polarization was observed in the cells of the studied species. *Halimeda cuneata* Hering cells are permanently polarized, with cortical cells and distinct medullary cells. The cortical cells exhibit vacuoles and a large number of chloroplasts, and the medullary cells contain large vacuoles, while amyloplasts, nuclei and other organelles are distributed throughout the medullary region [43].

Pit connections are structures of approximately 1 micrometer that are constricted in the middle and convex at the ends [44], as described for *H. musciformis* and other vegetative and reproductive algal cells [40,42,45,46]. The rhodophycean pit connection consists of two major components of the plug: the core and the cap, which differ in chemical composition. This structure is present in all members of the Florideophyceae and is reported to occur at one stage in the life cycle of two members of the Bangiophyceae [44].

Therefore, the morphology and ultrastructure of *H. cervicornis* and *H. musciformis* are fundamental to an understanding of algae adaptation, as well as provide insights on lectin function.

Many studies have reported on algal lectins; however, as with plant lectins, little is known about the biological role that lectins might have in marine algae. Hori et al. [14] suggested that marine algal agglutinins may play a common, but as yet unknown, physiological role in algae. Bolwell et al. [47,48] isolated a lectin-like protein from the sperm cell surface of the brown alga *Fucus serratus* L. (Ochrophyta) involved in specific gamete recognition. Other studies have characterized molecules with similar function in *Antithamnion sparsum* (Ceramiaceae, Rhodophyta) [21], *Aglaothamnion oosumiense* (Ceramiaceae, Rhodophyta) [49,50] and *A. callophyllidicola* [51]. Some studies characterized lectin as a fundamental molecule involved in protoplast regeneration of the marine coenocytic green algae *Bryopsis hypnoides* J.V. Lamouroux [22] and *Codium fragile* (Suringar) Hariot (Bryopsidales, Chlorophyta) [23]. Since they are present in different cell regions, our findings suggest that HML and HCL could play many physiological roles, such as cytoplasm aggregation and carbohydrates recognition on cell wall. Other studies have implicated lectins as biotechnological tools to delineate polysaccharides on the surfaces of algal spores [21,40,52]. Lectins are a class of proteins that specifically bind to carbohydrates and form complexes with molecules and biological structures containing saccharides, without altering the covalent structure of glycosyl ligands. These proteins are, in fact, potential tools for biotechnology. Therefore, it is important to investigate not only the sugar specificity but also the cross reaction of anti-lectin antibodies with other proteins. Lectins have been identified in many algal species [53], including HCL and HML that have particular characteristics that define a novel lectin family [54]. HML binds GalNAc/Gal substituted with a neutral sugar through 1–3, 1–4, or 1–2 linkages in O-linked mucin-type glycans and Fuc(α1–6)GlcNAc of N-linked glycoproteins [54].

Polysaccharides that constitute mucilage have also been detected using lectins conjugated with fluorescent proteins in *Gelidium floridanum* W.R. Taylor [40], *Laurencia arbuscula* Sonder [29], *Nemalion helminthoides* (Velley) Batters [52] and *Porphyra spiralis* var. *amplifolia* E.C. Oliveira & Coll [55].

The cross reaction between plant lectins and Diocleinae was previously described. Antibodies directed against *Dioclea altissima* lectins recognized not only different *D. altissima* fractions but also *D. grandiflora* lectins. Anti-*Canavalia brasiliensis* lectin (ConBr) IgG recognized *D. wilsonii* lectins (DWL) [56]. Our results confirm that HML must be a very distinct family of lectins as previously described [15,16,54].

Siphonaceous algal protoplasm can aggregate and regenerate into a mature individual in the absence of a cell membrane [57]. In *Bryopsis hypnoides* (Chlorophyta, Bryopsidaceae), organelle aggregation was mediated by a lectin-carbohydrate complementary system [22]. Enzyme treatment experiments on the assembly of *Codium fragile* (Suringar) Hariot (Chlorophyta, Bryopsidales) protoplasts indicated that proteinase K and a sea snail enzyme could block the aggregation of protoplasm. Thus, the substances involved in the formation of the protoplast might be composed of proteins and saccharides [23]. The distribution of HML and HCL throughout the cytoplasm and cell wall is consistent with this idea; however, immunocytochemical studies are needed to better understand lectin function. Marine alga lectins are especially interesting for biological applications because they have generally lower molecular weights compared with most plant lectins. These smaller molecules are expected to be less antigenic than the larger plant lectins [18].

5. Conclusion

The studied species presented, in transverse section, thalli with three regions of cells being the central cells with big vacuoles. Ultrastructure variations were noted, especially cell wall thickness. This is the first work elucidating the sublocalization of a lectin on red marine red algae by immunocytochemistry. The subcellular localization of a lectin in algal tissue, in particular, the presence of free lectin in the cytoplasm and cell wall, suggests that this protein might have multiple functions, providing a better

understanding of the physiological role of this protein and leading to the improvement of purification methods.

Conflict of interest

The authors have no conflict of interest to declare.

Acknowledgments

The authors would like to thank the Central Analítica-UFC/CT-INFRA/MCTI-SISNANO/Pró-Equipamentos CAPES and the Laboratório de Biologia Celular e Tecidual (UENF) for technical support. AHS, BSC, MC and KSN are senior investigators of CNPq (Brazil). The authors also thank CNPq–Conselho Nacional de Desenvolvimento Científico e Tecnológico (Process number 560350/2010-4), CAPES and FUNCAP.

References

[1] Guimarães SMPB, Horta PA. Morphology and reproduction of *Predaea feldmannii* Børgesen (Nemastomataceae, Rhodophyta), an uncommon species from Brazil. Rev Bras Bot 2004;2:507–13.
[2] Wolf AM, Sfriso A, Andreoli C, Moro I. The presence of exotic *Hypnea flexicaulis* (Rhodophyta) in the Mediterranean Sea as indicated by morphology, rbcL and cox1 analyses. Aquat Bot 2011;95:55–8.
[3] Dodge JD. The fine structure of algal cells. London, New York: Academic Press; 1973.
[4] Schmidt EC, Scariot LA, Rover T, Bouzon ZL. Changes in ultrastructure and histochemistry of two red macroalgae strains of *Kappaphycus alvarezii* (Rhodophyta, Gigartinales), as a consequence of ultraviolet B radiation exposure. Micron 2009;40:860–9.
[5] Lee RE. Phycology. 4 ed. UK: Cambridge University Press; 2008, 614 pp.
[6] Schmidt ÉC, Maraschin M, Bouzon ZL. Effects of UVB radiation on the carragenophyte *Kappaphycus alvarezii* (Rhodophyta Gigartinales): changes in ultrastructure, growth, and photosynthetic pigments. Hydrobiologia 2010;649:171–82.
[7] Lamouroux JVF. Essai sur les genres de la famille des thalassiophytes non articulées. Annales du Muséum d'Histoire Naturelle, Paris 20: 21–47, 115–139, 267–293, 7–13; 1813.
[8] Abbott IA, Norris JN. Taxonomy of economic seaweeds, vol. III California: La Jolla; 1992, 256pp.
[9] Ateweberhan M, Van Reine WFP. A taxonomic survey of seaweeds from *Eritrea*. Blumea 2005;50:65–111.
[10] Bitencourt FDS, Figueiredo JG, Mota MRL, Bezerra CCR, Silvestre PP, Vale MR, et al. Antinociceptive and anti-inflammatory effects of a mucin-binding agglutinin isolated from the red marine alga *Hypnea cervicornis*. Naunyn Schmiedebergs Arch Pharmacol 2008;377:139–48.
[11] Figueiredo JG, Bitencourt FS, Cunha TM, Luz PB, Nascimento KS, Mota MRL, et al. Agglutinin isolated from the red marine alga *Hypnea cervicornis* J. Agardh reduces inflammatory hypernociception: involvement of nitric oxide. Pharmacol Biochem Behav 2010;96:371–7.
[12] Reis RP, Caldeira AQ, dos Santos Miranda AP, Barros-Barreto MB. Potencial para maricultura da carragenófita *Hypnea musciformis* (Wulfen) J. V. Lamour. (Gigartinales – Rhodophyta) na Ilha da Marambaia, Baía de Sepetiba, RJ, Brasil. Acta Bot Bras 2006;20:763–9.
[13] Reis RP, Yoneshigue-valentin Y. Variação espaço-temporal de populações de *Hypnea musciformis* (Rhodophyta, Gigartinales) na baía de Setiba e Armação dos Búzíos, RJ, Brasil. Acta Bot Bras 1999;12:465–83.
[14] Hori K, Miyazawa K, Fusetani N, Hashimoto K, Ito K. Hypnins, low-molecular weight peptidic agglutinins isolated from a marine red alga *Hypnea japonica*. Biochim Biophys Acta 1986;873: 228–36.
[15] Nagano CS, Moreno FBMB, Bloch Jr C, Prates MV, Calvete JJ, Saker-Sampaio S, et al. Purification and characterization of a new lectin from the red marine alga *Hypnea musciformis*. Protein Pept Lett 2002;9:159–66.
[16] Nascimento KS, Nagano CS, Nunes EV, Rodrigues RF, Goersch GV, Cavada BS, et al. Isolation and characterization of a new agglutinin from the red marine alga *Hypnea cervicornis* J. Agardh. Biochem Cell Biol 2006;84:49–54.
[17] Sharon N, Lis H. Lectins as cell recognition molecules. Science 1989;246:227–34.
[18] Rogers DJ, Hori K. Marine algal lectins: new developments. Hydrobiologia 1993;260:589–93.
[19] Peumans WJ, Van Damme EJM. Lectins as plant defense proteins. Plant Physiol 1995;109:347–52.
[20] Cavada BS, Vieira CC, Silva LM, de Almeida Silva LM, de Oliveira JTA, de Azevedo Moreira R. Comportamento da lectina de sementes de *Canavalia brasiliensis* Mart. durante a germinação em presença de luz. Acta Bot Bras 1990;4:13–20.
[21] Kim GH, Lee IK, Fritz L. Cell–cell recognition during fertilization in a red alga, *Antithamnion sparsum* (Ceramiaceae, Rhodophyta). Plant Cell Physiol 1996;37:621–8.
[22] Niu J, Wang G, Lü F, Zhou B, Peng G. Characterization of a new lectin involved in the protoplast regeneration of *Bryopsis hypnoides*. Chinese J Oceanol Limnol 2009;27:502–12.
[23] Li D, Lü F, Wang G, Zhou B. Assembly of the protoplasm of *Codium fragile* (Bryopsidales, Chlorophyta) into new protoplasts. J Integr Plant Biol 2008;50:752–60.
[24] Reynolds ES. The use of lead citrate at high pH as an electron-opaque staining in electron microscopy. J Cell Biol 1963;17:208–12.
[25] Yamagishi Y, Masuda M. A taxonomic revision of a Hypnea charoides-valentiae complex (Rhodophyta, Gigartinales) in Japan, with a description of *Hypnea flexicaulis* sp. nov. Phycol Res 2000;48:27–35.
[26] Geraldino PJL, Yang EC, Kim MS, Boo SM. Systematics of *Hypnea asiatica* sp. nov. (Hypneaceae, Rhodophyta) based on morphology and nrDNA SSU, plastid rbcL, and mitochondrial cox1. Taxon 2009;58:606–16.
[27] Dawes CJ, Teasdale BW, Friedlander M. Cell wall structure of the agarophytes *Gracilaria tikvahiae* and *G. cornea* (Rhodophyta) and penetration by the epiphyte Ulva lactuca (Chlorophyta). J Appl Phycol 2000:567–75.
[28] Couto RP, Neto AI, Rodrigues AS. Metal concentration and structural changes in *Corallina elongata* (Corallinales, Rhodophyta) from hydrothermal vents. Mar Pollut Bull 2010;60:509–14.
[29] Bouzon ZL, Ouriques LC. Characterization of *Laurencia arbuscula* spore mucilage and cell walls with stains and FITC-labelled lectins. Aquat Bot 2007;86:301–8.
[30] Foltran A, Maranzana G, Rascio N, Scarabel L, Talarico L, Andreoli C. *Iridaea cordata* from Antarctica: an ultrastructural, cytochemical and pigment study. Bot Mar 1996;39:533–41.
[31] Trick HN, Pueschel CM. Cytochemistry of pit plug in *Bossiella californica*. Phycology 1990;29:403–9.
[32] Vairappan CS. Seasonal occurrences of epiphytic algae on the commercially cultivated red alga *Kappaphycus Alvarezii* (Solieriaceae, Gigartinales, Rhodophyta). J Appl Phycol 2006;18:611–7.
[33] Broadwater ST, LaPointe E. Parasitic interactions and vegetative ultrastructure of *Choreonema thuretii* (Corallinales, Rhodophyta). J Phycol 1997;407:396–407.
[34] Bouzon ZL, Ferreira EC, dos Santos R, Scherner F, Horta PA, Maraschin M, et al. Influences of cadmium on fine structure and metabolism of *Hypnea musciformis* (Rhodophyta Gigartinales) cultivated in vitro. Protoplasma 2011;249:637–50.
[35] Schmidt ÉC, Pereira B, dos Santos RW, Gouveia C, Costa GB, Faria GSM, et al. Responses of the macroalgae *Hypnea musciformis* after in vitro exposure to UV-B. Aquat Bot 2012;100:8–17.
[36] Abbas A, Shameel M. Anatomical studies on *Colpomenia sinuosa* (Phaeophycota) from Karachi coast of Pakistan. Pakistan J Bot 2009;41:1921–6.
[37] Abbas A, Shameel M. Anatomical studies on *Lonbophora variegata* (Phaeophycota) from the coast of Pakistan. Pakistan J Bot 2010;42:4169–76.
[38] Abbas A, Shameel M. Anatomy of *Dictyopteris divaricata* (Phaeophycota) from the coast of Karachi. Pakistan J Bot 2011;43:2207–10.
[39] Tsekos I. The supramolecular organization of red algal cell membranes and their participation in the biosynthesis and secretion of extracellular polysaccharides: a review. Protoplasma 1996;193:10–32.
[40] Bouzon ZL, Ouriques LC, Oliveira EC. Spore adhesion and cell wall formation in *Gelidium floridanum* (Rhodophyta, Gelidiales). J Appl Phycol 2006;18:287–94.
[41] Schmidt ÉC, dos Santos RW, de Faveri C, Horta PA, de Paula Martins R, Latini A, et al. Response of the agarophyte *Gelidium floridanum* after in vitro exposure to ultraviolet radiation B: changes in ultrastructure, pigments, and antioxidant systems. J Appl Phycol 2012;24:1341–52.
[42] Delivopoulos S. Ultrastructure of auxiliary and gonimoblast cells during carposporophyte development in the red alga *Cryptopleura*

ruprechtiana (Delesseriaceae, Ceramiales, Rhodophyta). Biol Cell 2003;95:383–92.
[43] Bouzon ZL, Bandeira-Pedrosa ME, Shimidt ÉC, Schmidt EC. Ultrastructure of the siphonaceous green alga *Halimeda cuneata*, with emphasis on the cytoskeleton. Micron 2010;41:598–603.
[44] Pueschel CM. A freeze-etch study of the ultrastructure of red algal pit plugs. Protoplasma 1977;91:15–30.
[45] Bouzon ZL, Schmidt EC, Almeida AC, Yokoya NS, Oliveira MC, Chow F. Cytochemical characterization and ultrastructural organization in calluses of the agarophyte *Gracilariopsis tenuifrons* (Gracilariales Rhodophyta). Micron 2011;42:80–6.
[46] Ashen JB, Goff LJ. Galls on the marine red alga *Prionitis lanceolata* (Halymeniaceae): specific induction and subsequent development or an algal – bacterial symbiosis. Am J Bot 1998;85: 1710–21.
[47] Bolwell GP, Callow JA, Evans LV. Fertilization in brown algae III. Preliminary characterization of putative gamete receptors from eggs and sperm of *Fucus serratus*. J Cell Sci 1980;43:209–24.
[48] Bolwell GP, Callow JA, Evans LV. Fertilization in brown algae II. Evidence for lectin-sensitive complementary receptors involved in gamete recognition in *Fucus serratus*. J Cell Sci 1979;36: 19–30.
[49] Kim S, Kim GH. Cell–cell recognition during fertilization in the red alga. Aglaothamnion Hydrobiol 1999;398/399:81–9.
[50] Han JW, Klochkova TA, Shim JB, Yoon K, Kim GH. Isolation and characterization of a sex-specific lectin in a marine red alga *Agloathamnion oosumiense* Itono. Appl Environ Microbiol 2012;78:7283–9.
[51] Shim E, Shim J, Klochkova Ta, Han JW, Kim GH. Purification of a sex-specific lectin involved in gamete binding of *Aglaothamnion callophyllidicola* (Rhodophyta). J Phycol 2012;48:916–24.
[52] Ouriques LC, Schmidt ÉC, Bouzon ZL. Cytochemical study of spore germination in *Nemalion helmintoides* (Nemaliales, Rhodophyta). J Adv Microsc Res 2011;6:81–8.
[53] Peumans WJ, Van Damme EJM. Peumans and van damme. Biotechnol Genet Eng Rev 1998;15:199–227.
[54] Nagano CS, Debray H, Nascimento KS, Pinto VPT, Cavada BS, Sakersampaio S, et al. HCA and HML isolated from the red marine algae *Hypnea cervicornis* and *Hypnea musciformis* define a novel lectin family. Protein Sci 2005;14:2167–76.
[55] Ouriques LC, Schmidt EC, Bouzon ZL. The mechanism of adhesion and germination in the carpospores of *Porphyra spiralis* var, amplifolia (Rhodophyta, Bangiales). Micron 2012;43:269–77.
[56] Moreira RA, Monteiro ACO, Horta ACG, Oliveira JTA, Cavada BS. Isolation and characterization od *Dioclea altissima* var megacarpa seed lectin. Phytochemistry 1997;46:139–44.
[57] Ye N, Wang G, Wang F, Zeng C. Formation and growth of *Bryopsis hypnoides* lamouroux regenerated from its protoplasts. J Integr Plant Biol 2005;47:856–62.